

Optimization of Photovoltaic Pumping System Controlled by EV80C196MC Microcontroller Evaluation Board Part-I

M. Arrouf, F. Benabid and N. Bouguachel

Department of Electrical Engineering, Faculty of Sciences and Engineering,
University of Batna, 05000 Batna, Algeria

Abstract: Due to rapid growth and declining cost of solar cells manufacturing as well as the progress of power electronics control techniques, photovoltaic energy is of increasing interest in pumping system applications particularly in the isolated area, such as in Batna region in Algeria. Obviously, Photo Voltaic Generators (PVG) are classified as non linear electrical sources since the output power is affected by the weather conditions such as insolation and temperature which changes randomly in time. Thus, the enhancement of the efficiency of the photovoltaic pumping system depends on the optimization of the electric energy generated by the photovoltaic generator. This study presents an optimally designed photovoltaic pumping system to work in the remote area of Batna region under the variation of climate conditions, it consists of: Maximum Power Point Tracking (MPPT), 3 phase Pulse Width Modulation inverter (PWM) Voltage Source Inverter (VSI) and induction motor actuating centrifugal pump. The system is governed by EV80C196MCS Microcontroller Evaluation Board. The photovoltaic pumping system is built at the laboratory level and the first tests have showed very promising results.

Key words: Photovoltaic generator, MPPT, inverter, induction motor, centrifugal pump

INTRODUCTION

The utilization of photovoltaic conversion to power water pumps is today an emerging technology, characterized by gradually declining costs. In remote area far away from national electric grid, the use of photovoltaic pumping system for irrigation is economically advantageous where the typical heads lie between 1-100 m (Duzat, 200). Algeria is a large area country about 2.4 millions km² with variety in sites leading to a diversity in climate. Solar energy represents a significant potential in Algeria. In fact the country receives more than 3000 h of sunshine per year with a high level of radiation. Due to this diversity in the climate, the average global insolation at the received horizontal plane varies between 4.5 and 7.5 kWh m⁻² (Capderou, 1986).

In this study a photovoltaic pumping system is optimally designed and realized to work in the remote area of Batna region under the climate conditions mentioned above, it is composed of: PVG, MPPT, three phases PWM voltage source inverter and induction motor actuating centrifugal pump. The optimization of the system is based upon the optimization of the power delivered by the PVG;

this is done by the MPPT and the optimization of the induction motor efficiency which is completed by the application of a nearly constant ratio voltage to frequency control technique.

System lay-out: The schematic diagram of the realized photovoltaic pumping system is proposed in Fig. 1. As shown in the figure, the system consists of a PVG which presents the supply source. A boost chopper that is used as an MPPT connected to a PWM inverter; which converts the DC power to an AC power in order to feed the three phase loaded induction motor.

The MPPT control strategy and the inverter PWM switching pattern are obtained from the developed program for this task implemented on the microcontroller.

Photovoltaic generator: A photovoltaic generator consists of a number of modules, formed by the interconnection of photovoltaic cells, connected together in series and parallel to provide the required voltage and current. The performance of the generator therefore depends on variability of the modules that comprise the generator and the cells that comprise the modules. Figure 2 represent the one diode model circuit of the photovoltaic cell.

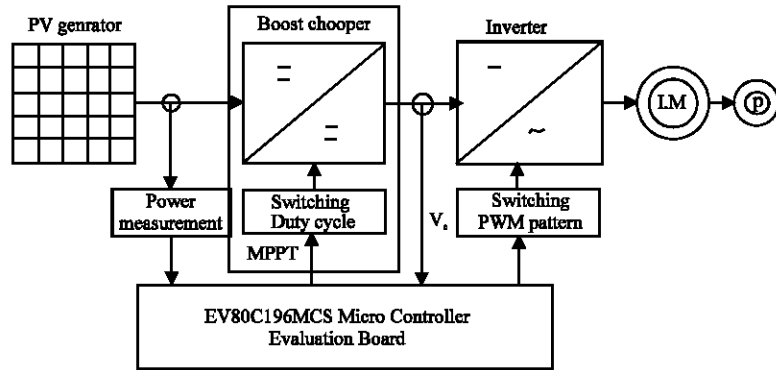


Fig. 1: Block diagram of PV pumping system

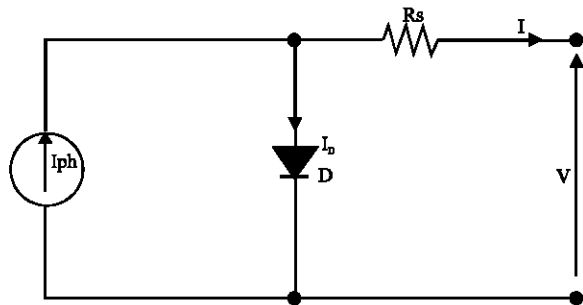


Fig. 2: Solar cell equivalent circuit

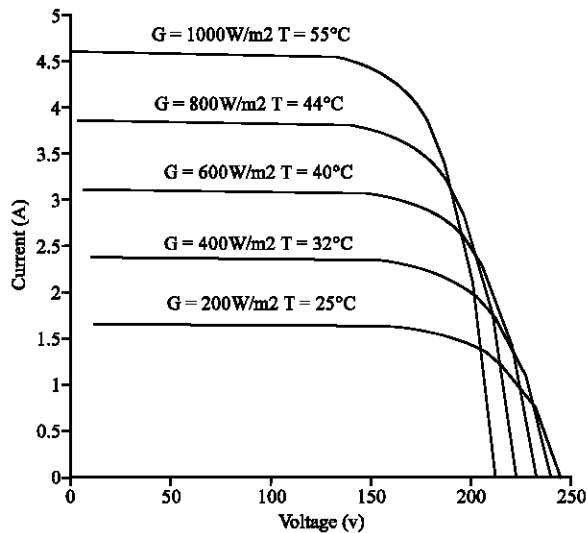


Fig. 3: I-V characteristics of PV generator

For a photovoltaic generator composed of N_p modules in parallel and N_s in series the I-V equation is given by:

$$I_g = N_p I_{ph} - N_p I_{sat} \left\{ \exp \left[\frac{q}{AKTN_s} (V_g + I_g R_s) \right] - 1 \right\} \quad (1)$$

where I_g and V_g are the output current and voltage of the PVG, respectively, I_{ph} is the generated current under a given insolation, I_{sat} is the saturation current of the photovoltaic generator, q is the charge of electron, K is the Boltzman's constant, R_s is the series resistance and A is the ideality factor for the P-N junction.

Figure 3 shows the power- voltage I-V characteristics of a photovoltaic generator as a function of solar irradiance and temperature and Fig. 4 shows the P-V characteristics.

MAXIMUM POWER POINT TRACKING

The MPPT is the essential element in the optimization of photovoltaic pumping systems since the PVG is a non-linear energy source. In order to optimize the electrical operating conditions of the generator, it is necessary to use an MPPT which consists of: A power section and a control section. The power section is generally a DC/DC converter whereas the control section can be constructed either by logic or analog electronics.

Two types of DC/DC converters topologies, buck converter or boost converter, are the most commonly used by the majority of designers of maximum power tracking. In our case the step-up converter is designed since it has excellent characteristics such as high efficiency, high-voltage output capability, constant dc-array current, small size and low cost (Glasner, 1996).

The step-up converter is used to truly track the maximum power point rather than maximizing the voltage. The basic circuit of the step-up converter designed and developed is shown in Fig. 5; where the MOSFET is used as a switching device because for its ease of control, high efficiency and fast switching speed. The input inductor is wound on a ferrite-core with air-gap to prevent core saturation that might be caused by a large DC current component value.

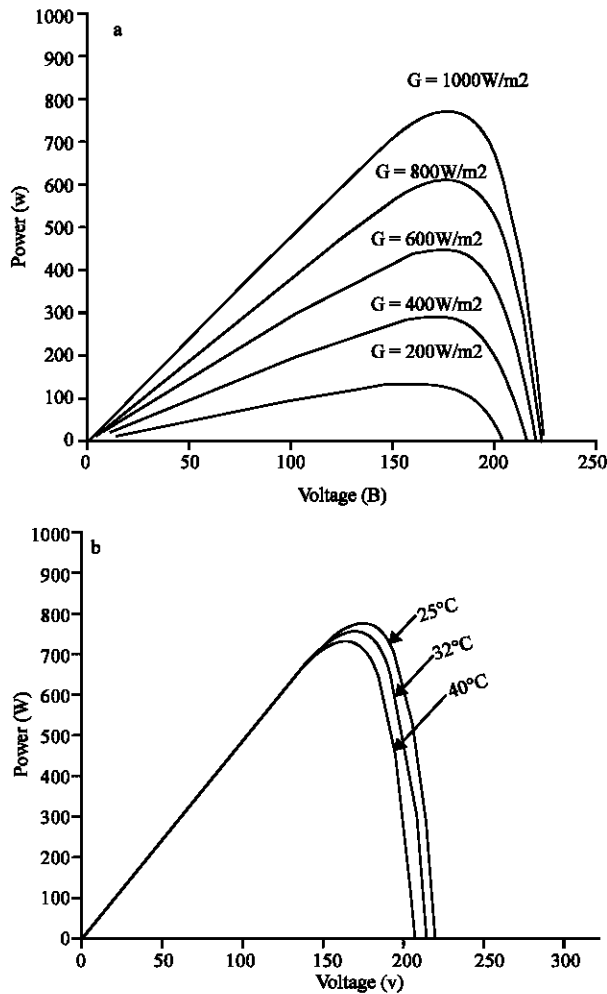


Fig. 4: Power-Voltage Characteristics of PVG (a) for five insolation levels (b) three temperatures (cross sign marks the maximum power point)

It is well known that the relationship between the input voltage and the output voltage of the step-up converter is given by:

$$V_{out} = (1/1 - \alpha) V_{pv} \quad (2)$$

where $\alpha = t_{on}/T$ is defined as the converter duty cycle. This means that the converter output voltage can be simply controlled by the variation of the duty cycle α .

The inductor value, L , required to operate the converter in the continuous conduction mode is calculated such that the peak inductor current at maximum output power does not exceed the power switch current rating. Hence, L is calculated as:

$$L \geq (V_{pv} \alpha / f_s \Delta I_{pv}) \quad (3)$$

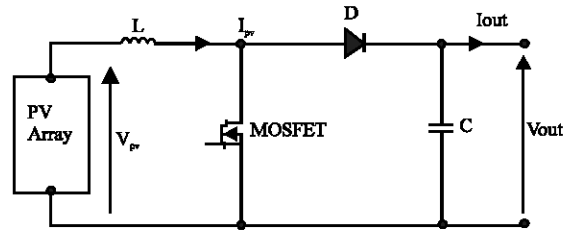


Fig. 5: Step-up chopper

where $f_s = 1/T_s$ is the switching frequency, α is the duty cycle at maximum converter output power, V_{pv} the input voltage and ΔI_{pv} is the peak-to-peak inductor ripple current.

The choice of the converter inductor value and the switching frequency is a compromise between converter efficiency, cost, power capability and weight.

The output capacitor value calculated to give the desired peak-to-peak output voltage ripple is given by:

$$C \geq (I_{out} \alpha / f_s \Delta V_{out}) \quad (4)$$

Where $f_s = 1/T_s$ is the switching frequency, I_{out} is the output current and is the ΔV_{out} peak-to-peak ripple of the capacitor output voltage.

TRACKING TECHNIQUE

Several techniques have been proposed in order to drive an AC or DC loads at the MPP. These techniques are based on the regulation of the PVG output voltage or current according to a reference voltage or current signal, which either constant or derived from the PV generator characteristics. A distinction of these techniques is to directly use the DC/DC converter duty cycle as a control parameter and force the derivative to zero, where is the PVG output power and is the duty cycle, therefore only one control loop is required as illustrated in Fig. 6 (Weindong, 2004).

In the technique proposed, an EV80C196MCS Microcontroller Evaluation Board is used as a tool of control of the PVG output power and the duty cycle of the DC/DC converter. This is done through the reading of the instantaneous PVG output voltage and current, then the power is calculated and compared to the previous PVG output power.

Depending on the result of the comparison the duty cycle is changed accordingly and the process is repeated until the maximum power point has been reached. The proposed technique could be easily implemented also with analog circuits, instead of using an EV80C196MCS

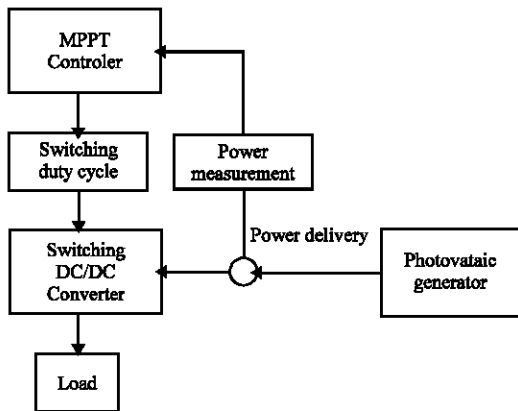


Fig. 6: The block diagram of the MPPT control system

Microcontroller Evaluation Board, but the utilization of such board has the advantage that it can also generate the PWM driving signals of the inverter in the photovoltaic pumping system proposed chain. Moreover, it permits easy modification if additional renewable energy sources are used.

The system control unit based on the EV80C196MCS Microcontroller Evaluation Board which consists of (1992)

- Intel’s 80C196MCS low power consumption, CMOS microcontroller with external EPROM and RAM.
- Interface circuits which contain sensors and signal conditioners connected to the microcontroller A/D converter.
- IC driver for the power MOSFET.

This type of Microcontroller was chosen because it has the necessary features for the proposed system, such as an on-chip A/D converter, PWM outputs, 16-bit architecture, high clock rate, low power consumption and low cost.

The flowchart of the control program is shown in Fig. 7. The incrementation or the decrementation of the duty cycle α either with (+d) or (-d) indicates the direction that must be followed on the P- α relationship curve, where P is the PVG power output and α is the duty cycle of a switching mode DC/DC converter. Since an 8-bit CPU register is used to store the PWM duty cycle in the present application, the value of α is made equal to 1/256. Initially, the duty cycle α is incremented with the value. In each iteration, the DC/DC converter input voltage and current are measured and the input power is calculated. The input power is compared to its value calculated in the previous iteration and according to the result of the comparison; the duty cycle is either incremented or decremented with the number d. Then, the

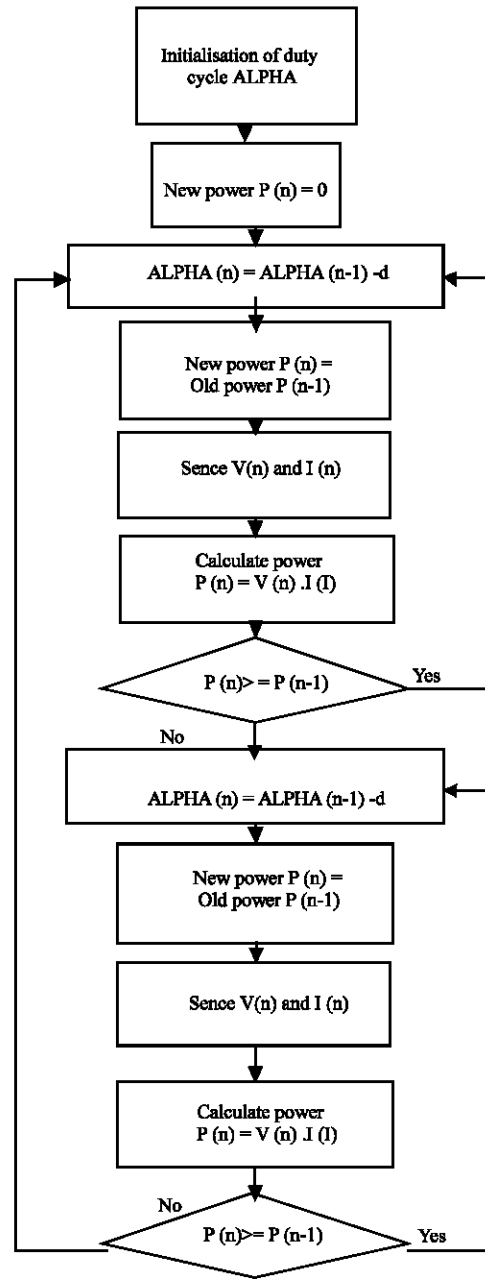


Fig. 7: The flowchart of the MPPT control technique

PWM output duty cycle is changed accordingly. The MPP tracking process is shown in Fig. 8. The starting point vary, depending on the atmospheric conditions, while the duty cycle is changed continuously, according to the above mentioned algorithm, resulting in the system steady state operation around the maximum power point.

Voltage source inverter: The voltage source inverter shown in Fig. 9 is used to convert the dc voltage into three-phase ac voltage and to supply the induction motor

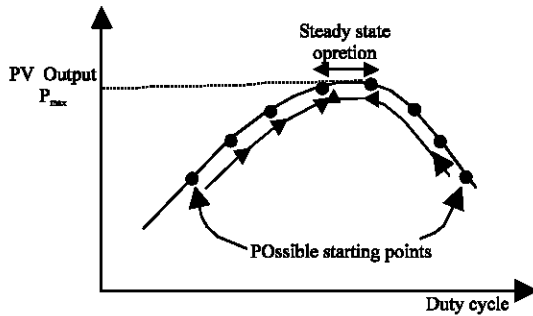


Fig. 8: MPPT tracking process

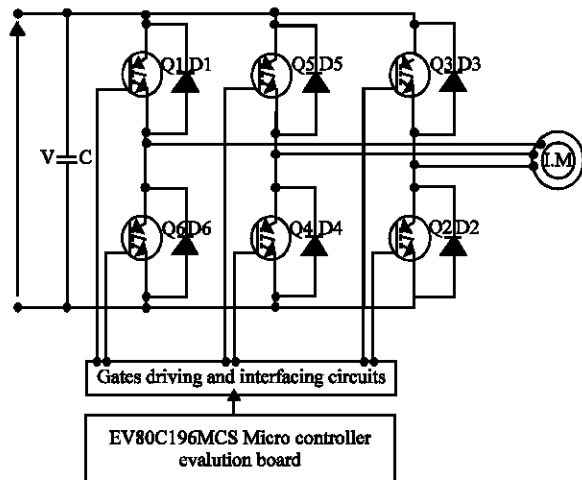


Fig. 9: Voltage source inverter

driving a centrifugal pump. The utilized Mitsubishi Intelligent Power Module PM10CSJ060 inverter is isolated base module designed for power switching application at frequencies up to 20 kHz with a built-in control circuits provide optimum gate drive and protection for IGBT and free-wheel power devices. The intelligent power module is specially designed for variable speed motor control and is characterized with high frequency and high efficiency operation. The inverter output voltage is controlled with a sinusoidal pulse-width modulation control technique in which a high frequency symmetrical triangular carrier wave is compared with a synchronized sine wave modulating reference wave with the required output frequency.

The sinusoidal PWM control technique is generated by the microcontroller in such away that the inverter output voltage frequency ratio is maintained constant. Due to the fluctuation of the maximum input power produced by the photovoltaic generator through the MPPT according to the solar radiation level and temperature the inverter output power is variable. The efficiency of the inverter ranges from 90 to 95%.

INDUCTION MOTOR OPERATION

To produce a starting torque and subsequently a running torque, it is necessary to have a current flowing through the rotor winding by short-circuiting the winding.

Initially the induced emf from the inverter causes a rotor current per phase I_R to flow through the short-circuit, producing an ampere conductor distribution that acts with the flux field to produce the starting torque. The flux field is assumed to revolve at a speed corresponding to the applied stator frequency and the poles of the stator winding. This speed is called the synchronous speed and is given by:

$$\omega_s = 2\omega/P \tag{5}$$

Where ω is the stator or source frequency in rad/s and P is the number of poles. The relative speed between the rotor and the flux wave or the slip is defined by.

$$S = (\omega_s - \omega_r) / \omega_s \tag{6}$$

Where ω_r is the operating speed of the motor .

Using the equivalent circuit of the induction motor shown in Fig.10 the torque equation is given by Murphy (1988).

$$T = 3Pk \frac{\omega_r X_m^2 / R_R}{\left[R_s - \frac{\omega_r}{S R_R} (X_{11} X_{22} - X_m^2) \right]^2 + \left[X_{11} + \frac{\omega_r R_s X_{22}}{\omega_s R_R} \right]^2} \tag{7}$$

Where K is the terminal voltage frequency ratio, p is the number of pole pairs, ω_r is the rotor frequency $S\omega_s = X_{11} = X_m + X_s$, $X_{22} = X_m + X_r$, X_m = mutual reactance at rated supply frequency, X_s , X_r = stator and rotor leakage reactances, respectively and S is the motor slip.

The input impedance is given by:

$$Z_{in} = \sqrt{(R_{in}^2 + X_{in}^2)} \tag{8}$$

$$R_{in} = R_s R_R^2 / S^2 + R_R X_m^2 / S + R_s X_{22}^2 / (R_R^2 / S^2 + X_{22}^2), \tag{9}$$

$$X_{in} = X_{11} R_R^2 / S + X_{11} X_{22}^2 - X_{22} X_m^2 (R_R^2 / S^2) + X_{22}^2 \tag{10}$$

The motor input current and power factor are given by:

$$I_{in} = V_s / Z_{in} \tag{11}$$

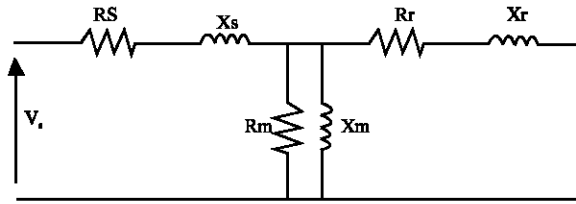


Fig. 10: Induction motor equivalent circuit

$$PF = \cos(\tan^{-1} X_{in} / R_{in}) \quad (12)$$

The input power is:

$$P_{in} = 3V_s I_s PF \quad (13)$$

The mechanical output power is:

$$P_m = (1 - S)\omega_s T \quad (14)$$

Hence,

$$\eta = P_m / P_{in} \quad (15)$$

The speed of the induction motor can be controlled by changing the supply frequency. Nevertheless the terminal voltage can be considered proportional to the product of frequency and the flux. If the voltage is maintained fixed at its rated value while the frequency is reduced below its rated value, the flux will increase. This would cause saturation of the air-gap flux. At low frequency the reactance will decrease and the motor current may be too high. In order to avoid saturation and to minimize losses, motor is operated at rated air-gap flux by varying terminal voltage with frequency so as to maintain the ratio of voltage to frequency nearly constant (Onhishi, 1988; Arrouf, 2003).

For the motor optimum efficiency operation, the ratio of the supply voltage applied to the induction motor and its frequency (V_s / ω_s) is adjusted in order to operate the motor at highest efficiency.

From the equivalent circuit, the total mechanical power of a motor is given by:

$$P_m = 3I_R^2 R_R (1 - S) / S \quad (16)$$

Hence,

$$\eta = [I_R^2 R_R (1 - S) / S] / I_s^2 R_{in} \quad (17)$$

By differentiating the efficiency expression with respect to the slip S , and equating to zero, an optimum slip which yields the maximum efficiency is obtained and given by:

$$S_{op} = (R_R / X_m + X_r) \sqrt{(1 + A)} / (1 + R_R / R_s) \quad (18)$$

where $A = X_m^2 / R_s R_m$ and is R_m the core loss resistance.

Motor operation at implies that the input impedance, the power factor and the motor efficiency are constant. The optimum mechanical speed is given by:

$$\omega_{mop} = (1 - S_{op}) \omega_s / p \quad (19)$$

Centrifugal pump: The pump represents the mechanical load of the induction motor and its size identifies the power rating of the other system component. The utilized pump is single stage centrifugal submersible one which can be characterized by the following equations (Abdel-Karim, 2005).

$$P_p = \rho g H Q \quad (20)$$

$$\eta_p = P_p / P_{mech} \quad (21)$$

Where P_p is the hydraulic output power of the pump in W , ρ is the water density in $kg\ m^{-3}$, g is the gravitation acceleration in $m\ s^{-2}$, Q is the flow rate in m^3/h , H is the pumping head in meters m , η_p is the pump efficiency and P_{mech} is the input mechanical power of the pump.

RESULTS AND DISCUSSION

To illustrate the performance of the designed and implemented system at the laboratory level, partial test have been carried out on the system in order to verify the well operation of the MPPT tracking process algorithm and the inverter output wave forms; generated by the PWM implemented program on the microcontroller, as well as the motor supply voltage and line current.

Figure (11a-e) show the evolution of the duty cycle of the PWM control signal of the boost chopper as the photovoltaic generator power increase or decrease. The variation of the power extracted from the PV generator due to the change of the duty cycle can be observed on the PC screen shown in Fig. 12a-e. In the program running by EV80C196MCS Microcontroller Evaluation Board connected to the PC the duty cycle is denoted 'ALPHA' while the power is denoted 'PUISSANCE'. For example in Fig. (12b) we can read ALPHA = 58 and PUISSANCE = 200 whereas, in Fig. (12c) we can read ALPHA = 98 and PUISSANCE = 316.

CONCLUSION

A photovoltaic pumping system controlled by an EV80C196MC Microcontroller Board has been described. The microcontroller has the functions of the generations of PWM signals of the inverter gate drive circuit as well as the control signal of the maximum power point tracking. The power electronics part of the photovoltaic pumping system and their devices gate driving circuit where optimally designed, realized and tested as shown in Fig. 15. The preliminary laboratory test results of the overall system where found to agree well with the predicted performance. More tests will be carried out on the field and the results will be published in a separate study.

Fig. 13: Induction motor line to line voltage

Fig. 14: Induction motor line current

Fig. 15: Realized PV system

From the five values of the duty cycle alpha and power that can be read on the screen of the PC in Fig. 12, it can be concluded that the tracking process of the PV power by the implemented MPPT is operating correctly.

Figure 13 shows the PWM wave form of the inverter output voltage which supplying induction motor, it can be seen from the Figure that the inverter is operating properly. Figure 13 shows the line current of the induction motor supplied from the PWM inverter, from the figure once can say the motor current is sinusoidal.

ACKNOWLEDGEMENT

I would like to thank Mr.M.Bouhrik for his help during the preparation of this study.

REFERENCES

- Abdel-Karim, D., 2005. Solar Powered Induction motor-driven Water Pump operating on a desert Well, simulation and field tests, *Renewable Energy*, pp: 701-714.
- Arrouf, M., 2003. Vector control of induction motor fed by photovoltaic generator, *Applied Energy*, 74: 159-169.
- Capderou, M., 1986. Atlas solaire de l'Algérie. T3 Aspect géométrique, synthèse géographique, Office des Publications Universitaires, Alger, Vol. 2.
- Duzat, R., 2000. Analytic and experimental investigation of a photovoltaic pumping system, PhD- work, Oldenburg University Dissertation.
- EV80C196MC Microcontroller Evaluation Board, User's Manual., 1992.
- Glasner, I., 1996. Advantage of boost VS. Buck topology for maximum power point tracker in photovoltaic system, *IEEE.*, pp: 356-358.
- Murphy, J.D., 1988. *Power Electronics Control of AC Motors*, Pergamon Press, Oxford.
- Ohnishi, T., 1988. High efficiency drive of an Induction Motor by means of V/F ratio control, *IECON, IEEE.*
- Weindong, X., 2004. A modified hill climbing MPPT method for photovoltaic power systems, 35th Ann. *IEEE. Power Elec. Specialists Conf.*, pp: 1957-1964.